

# Variable-Angle Directional Emissometer for Moderate-Temperature Emissivity Measurements

A. R. Ellis, H. M. Graham\*, Michael B. Sinclair, J. C. Verley

Sandia National Laboratories, PO Box 5800, Albuquerque, NM 87185

\*Lockheed Martin Aeronautics Company, Lockheed Blvd, Ft. Worth, TX 76108

## ABSTRACT

We have developed a system to measure the directional thermal emission from a surface, and in turn, calculate its emissivity. This approach avoids inaccuracies sometimes encountered with the traditional method for calculating emissivity, which relies upon subtracting the measured total reflectivity and total transmissivity from unity. Typical total reflectivity measurements suffer from an inability to detect backscattered light, and may not be accurate for high angles of incidence.

Our design allows us to vary the measurement angle ( $\theta$ ) from near-normal to  $\sim 80^\circ$ , and can accommodate samples as small as 7 mm on a side by controlling the sample interrogation area. The sample mount is open-backed to eliminate shine-through, can be heated up to 200 °C, and is kept under vacuum to avoid oxidizing the sample. A cold shield reduces the background noise and stray signals reflected off the sample. We describe the strengths, weaknesses, trade-offs, and limitations of our system design, data analysis methods, the measurement process, and present the results of our validation of this Variable-Angle Directional Emissometer.

**Keywords:** emissivity, emissometer, thermal emission, reflectivity

## 1. MOTIVATION

Initial construction of the variable-angle directional emissometer (VADE) was undertaken to investigate claims of narrow-band, super-plankian emission from 3-D photonic-crystal materials<sup>1</sup>. Through refinements, the VADE has grown into a tool capable of measuring emissivity of a material over a wide range of angles, and at moderate temperatures, for better correlation to room temperature reflectivity and transmissivity measurements.

The initial design focused on understanding the error caused by inability to accurately measure the surface temperature of our relatively fragile tungsten logpile photonic-crystal structures. Direct temperature measurement techniques that were tried were either too destructive or not sufficiently accurate due to thermal gradients. We needed a way to determine a sample's emissivity without relying on error-prone temperature measurements. Our solution was to design a relative measurement system that places a well-understood reference material and the sample of interest in a thermally uniform environment. The resulting set of signals can then be used to calculate the emissivity. This is in contrast to a typical system where a calibrated blackbody is used as a reference and the sample temperature must be carefully measured for signal comparison. Using our relative measurement method, we do not need to be concerned about the exact temperature of our material as long as the reference and sample are truly at the same temperature.

## 2. EXPERIMENTAL SETUP

The VADE system (see optical diagram in Figure 1 and photograph in Figure 4) consists of a vacuum chamber and a Fourier-transform infrared spectrometer (FTIR) used as a computer-controlled interferometer and detector. The sample is mounted in a  $10^{-6}$  Torr vacuum chamber to reduce conductive heat losses and to avoid oxidation of our samples while

heating, and can be heated to operating temperatures up to 250 °C. The heater block is mounted on a rotary-linear motion arm that allows 360° rotation as well as height adjustment so the position of the sample can be changed while under vacuum. The heater block is a low-emissivity, gold-coated copper block (with a nickel diffusion barrier) with imbedded cartridge heaters. A top plate clamps the samples in place, and is designed so the samples are not shadowed at high angles.

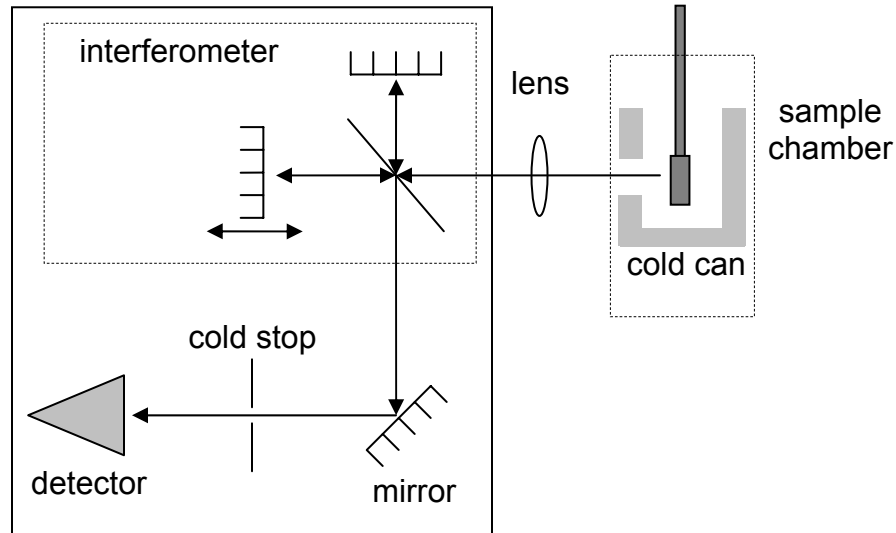


Figure 1: Layout of components in VADE system

We have developed two variations of the heater block: one with a solid back for opaque materials, and one with slots to reduce/remove shine-through from the heater. Both heater designs use thermocouples mounted at the top and bottom as feedback to the heater controller, and as a rough check of the temperature uniformity. Sketches of the two types of heater block are in Figure 2.

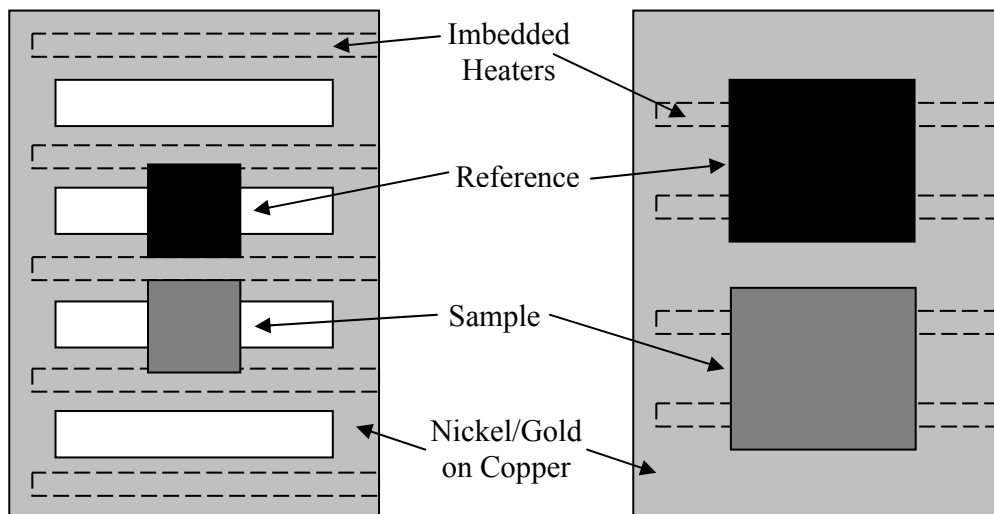


Figure 2: Two heater plate designs: five heaters for multiple samples (open-backed, left) and four heaters for a single, larger sample (closed back, right). For clarity, the top plates are not shown.

The vacuum chamber has a potassium-chloride optical window, coated with Parylene to reduce water absorption. A potassium-bromide plano-convex lens couples radiation from the material surface in the chamber to the emission port of a Thermo-Electron Nexus 6700 FTIR. The FTIR uses a high-sensitivity HgCdTe detector to provide spectrally-resolved data from 2 to 15  $\mu\text{m}$ . We use two shielding methods to limit the collection of unwanted signals: a cold can surrounding the heater and sample cooled by a helium cryogenic refrigerator, and a field-stop mounted in a liquid-nitrogen cryostat at the image plane in the FTIR sample compartment. The cold can is made of copper, with an exterior plated with gold on nickel to reflect background signals from the chamber, and an interior coating of flat-black paint to absorb light reflected by the sample and the heater plate. The cold field-stop limits the detector's field of view of background signals and reduces the area of the sample seen by the detector, which is particularly important for high-angle measurements. The maximum measurement angle ( $\theta_{\text{MAX}}$ ) for a given field-stop width is the highest angle the sample can be rotated such that the detector will not receive a signal from regions beyond the edges of the sample. With unit magnification,  $\theta_{\text{MAX}}$  is given by the expression,

$$\theta_{\text{MAX}} = \cos^{-1} (w/d), \quad (1)$$

where “w” is the width of the cold field stop, and “d” is the width of the sample. There must be no clipping of the emission from the sample by the heater block and top plate, and the field-stop must be imaged correctly on the center of the sample. If the sample is possibly off-center, an effective sample width (smaller than actual) should be used to be sure the leading edge of the sample is not visible to the detector. Figure 3 is a geometrical representation of the projection of the cold stop onto the tilted sample.

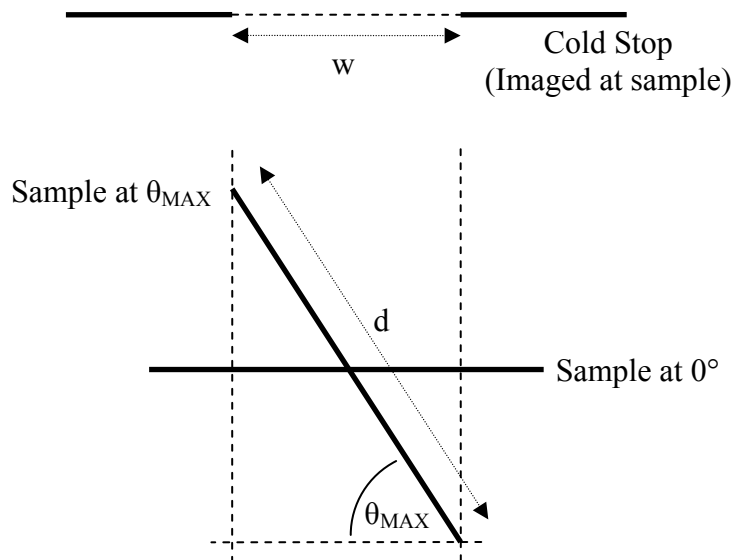


Figure 3: Geometrical representation to show how the cold stop aperture (w) limits the maximum angle ( $\theta$ ) obtainable for a given sample size (d).

The system may be signal-starved for small samples with low emissivities measured at high-angles from normal. Useful measurements have been made between 10° and 80°. With great care, higher-angle measurements may be possible. Another consideration for the spot size is the thickness of the sample. The heater plate is attached to a rotation arm, and it is designed so that the rotation is about the face of the sample of a given thickness (~670  $\mu\text{m}$ , the typical thickness of substrates for our photonic-crystal materials). If the sample is much thicker, or much thinner, the emitting area of the sample seen by the detector will shift significantly with angle. This shift must be calculated to avoid detecting emission from the edges of the sample at high angles.

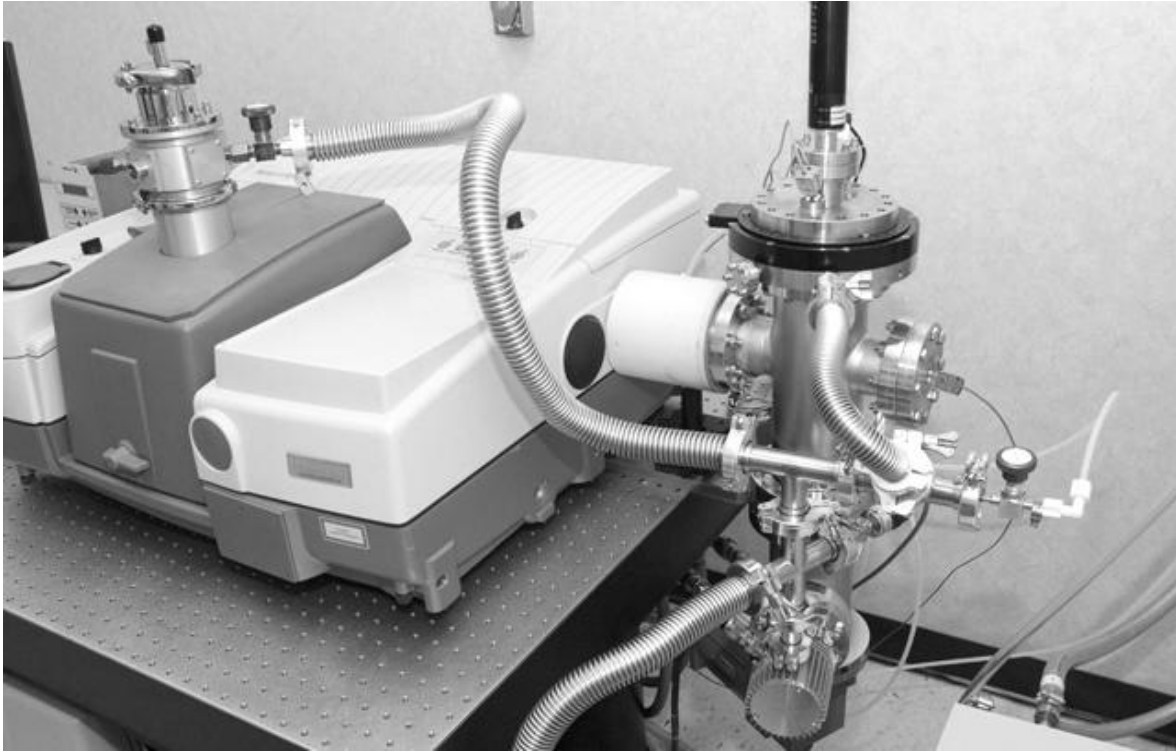


Figure 4: Photo of variable-angle directional emissometer

### 3. EMISSIVITY CALCULATION

To calculate the emissivity for an unknown sample at a given angle,  $\theta$ , we must measure signals from the reference and sample at two different temperatures,  $T_1$  and  $T_2$ , where  $T_2 > T_1$ . The measured signal,  $S$ , is the sum of three component sources (material emission, background emission, and sample reflections of background emission) modified by the responsivity of the optical path and the detector itself<sup>2</sup>:

$$S_{SA}(\lambda, \theta, T) = R(\lambda) * [\epsilon_{SA}(\lambda, \theta) * P(\lambda, T) + BG(\lambda) + I_{SA}(\lambda, \theta)] \quad (2)$$

$$S_{REF}(\lambda, \theta, T) = R(\lambda) * [\epsilon_{REF}(\lambda, \theta) * P(\lambda, T) + BG(\lambda) + I_{REF}(\lambda, \theta)]. \quad (3)$$

The responsivity of the system is “R”, “ $\epsilon$ ” is emissivity, “P” is Plank’s radiation equation, “BG” is the component from background sources, and “I” is the component reflected from the sample. “SA” and “REF” denote values for the sample and reference respectively.

Subtracting the two signals for a given material at different temperatures removes the background and reflection terms, as they are temperature independent. Then, a ratio of this difference signal of the sample to that of the reference yields an equation which relates the emissivities of the reference and sample to the four signals made in our measurement:

$$\epsilon_{SA}(\lambda, \theta) / \epsilon_{REF}(\lambda, \theta) = [S_{SA}(\lambda, \theta, T_2) - S_{SA}(\lambda, \theta, T_1)] / [S_{REF}(\lambda, \theta, T_2) - S_{REF}(\lambda, \theta, T_1)] \quad (4)$$

From equation 4, we can see that the accuracy of this method depends on the temperature uniformity between the sample and reference, the measurement accuracy of the reference's emissivity, the stability of the background signal, and the constancy of emissivity and reflectivity for both the sample and reference between  $T_1$  and  $T_2$ . A material that has a temperature-dependent emissivity will give a result that is an average for the temperature range; however, the emissivity of most materials does not vary appreciably in the 100-300 °C range.

#### 4. REFERENCE MATERIAL

This approach requires a reference material that has an independently-known emissivity at all angles, wavelengths, and temperatures of interest. Also, the requirement that the sample and reference temperatures must be the same during the measurement implies that the substrate of the reference must be identical in dimensions and in thermal properties. Therefore, we minimize temperature difference errors by using identical substrates for the sample and reference. The reference substrate is uniformly coated with a thin layer of high-emissivity paint. Our coating of choice is Krylon Flat Black spray paint, which we have found to be stable enough for moderate temperature use on most substrates.

The next challenge is to determine the emissivity of the reference material with a high level of accuracy. We are unaware of any established emissivity calibration methods for off-normal angles, so we must use an indirect method. Since the reference surface is isotropic and highly uniform, we can deduce the emissivity by making total transmissivity and total reflectivity measurements (using a calibrated gold standard), and subtracting these from unity following Kirchhoff's Law:

$$\varepsilon(\lambda, \theta, T) = 1 - R_{\text{TOTAL}}(\lambda, \theta, T) - T_{\text{TOTAL}}(\lambda, \theta, T). \quad (5)$$

We measure the total reflectivity and transmissivity of the reference material using a Surface Optics SOC-100 Hemispherical Directional Reflectometer (HDR)<sup>3</sup>. The benefit of using this system is that we can measure a wide range of angles (manufacturer specifies 7° to 80°), and the sample can be heated from room temperature up to about 500 °C. This gives us a large parameter space so we can match the conditions to those of the VADE measurement. We found the emissivity of our Krylon painted reference to be greater than 90% for angles up to 60°, and only slightly lower for higher angles, at wavelengths between 2 and 15 μm.

#### 6. VALIDATION TESTING AND EXPERIMENTAL DATA

To validate our system, we compared our direct emissivity data to deduced emissivity values ( $\varepsilon = 1-R$ ) from two different reflectometers: the SOC-100 HDR and a BOMEM DA3 FTIR system coupled with an 8" integrating sphere as a directional hemispherical reflectometer (DHR). As a test material, we chose a uniformly-oxidized aluminum coupon that has an emissivity that varies strongly as a function of wavelength between 2-15 μm, but has little temperature dependence. This material is also opaque at these wavelengths, obviating the need for transmission measurements. In the VADE, the sample was measured at temperatures of 130 °C and 150 °C, and all three systems collected data for angles 20°, 40°, 60°, 70°, 75°, and 80°.

In the BOMEM system, the sample is mounted in the middle of the integrating sphere at an angle,  $\theta$ , for DHR measurements as shown in Figure 5. Light scattered by the sample is collected at the exit aperture and sent to the FTIR detector.

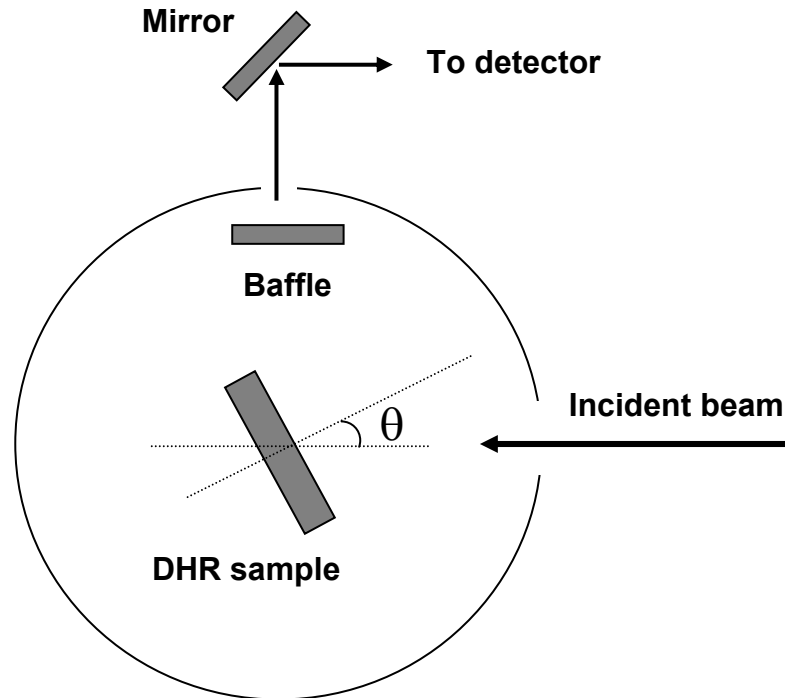


Figure 5: BOMEM integrating sphere configurations for DHR or DHT measurements

The HDR (Figure 6) uses a specular gold-coated ellipsoidal dome as a  $2\pi$  steradian mirror that collects light from a heated cavity at one focus and uniformly illuminates the sample at the second focus. The signal from the sample is collected by an overhead mirror that redirects the radiation into an FTIR. The use of this system was described in a previous paper.<sup>4</sup>

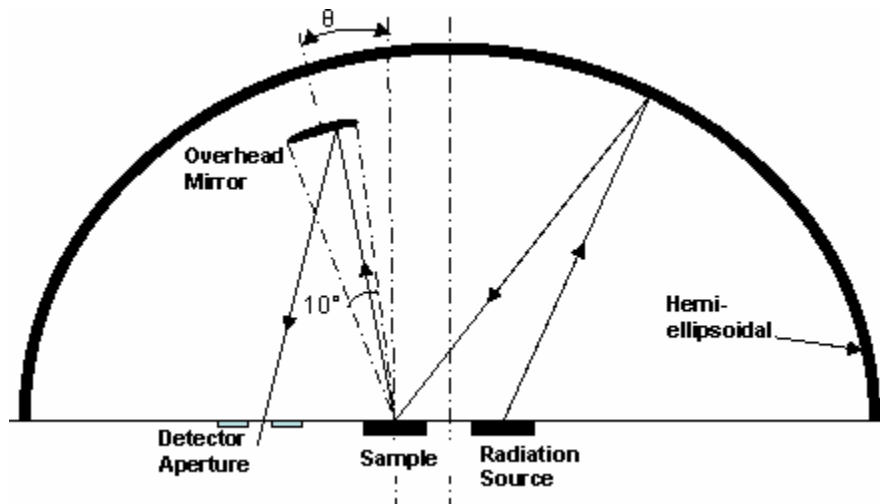


Figure 6: Geometry of SOC-100 used to measure HDR

The results from the three systems are quite consistent and are within 5% across the sensitive spectral range for most of the data. As we increased angle, a larger, narrow-band discrepancy developed between the HDR and the closely-matched DHR and VADE data around  $6 \mu\text{m}$ . The DHR measurements were unreliable above  $70^\circ$ , thus limiting our comparison of  $75^\circ$  and  $80^\circ$  data. Below, we show a subset of the data at  $20^\circ$ ,  $70^\circ$ , and  $80^\circ$  in Figures 7, 8, and 9.

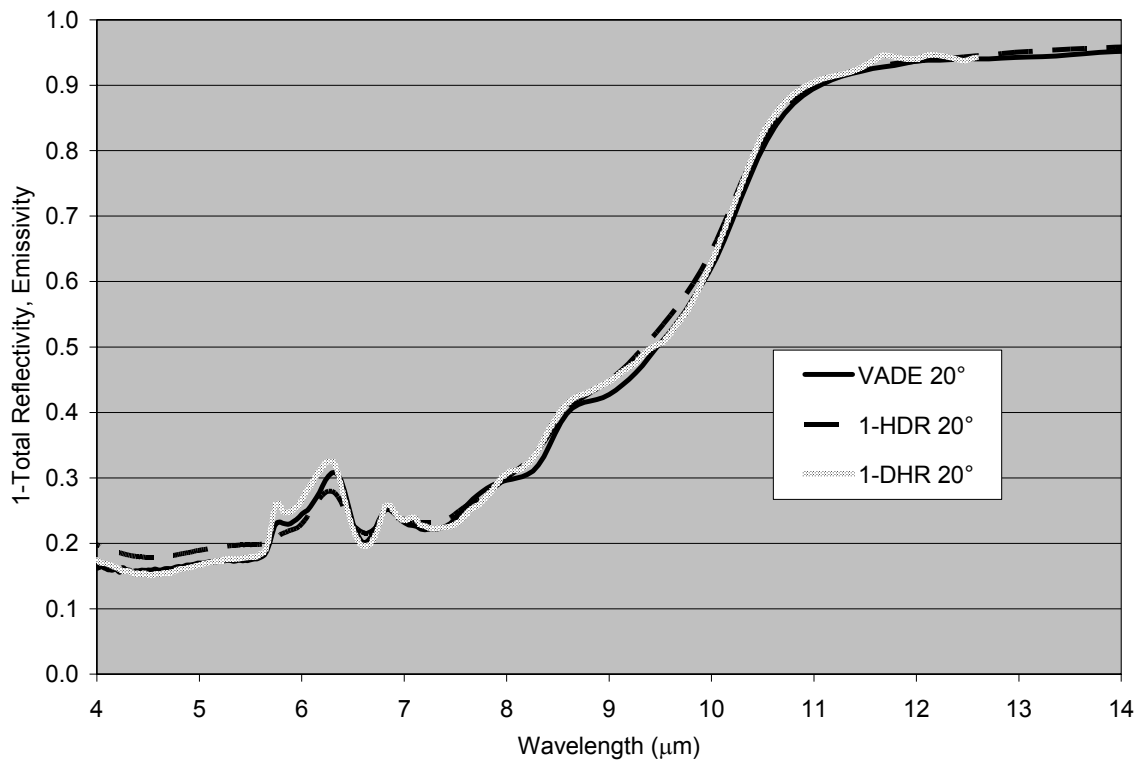


Figure 7: Comparison of oxidized aluminum data from VADE, HDR, and DHR systems at 20°

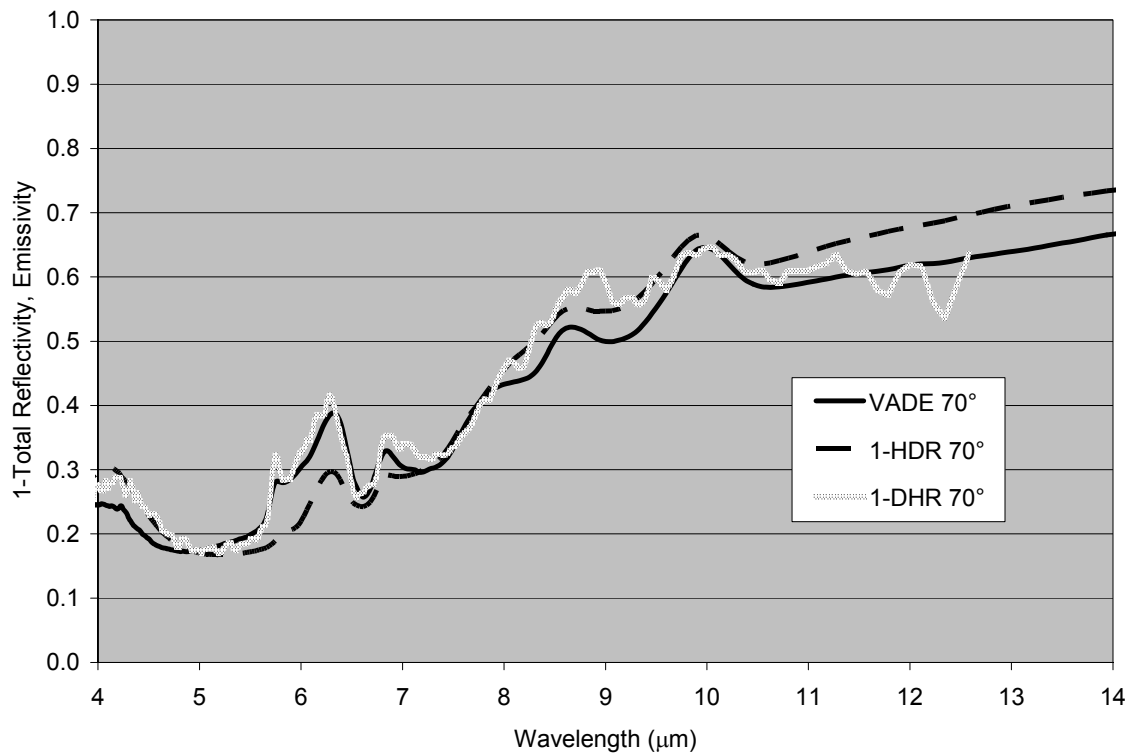


Figure 8: Comparison of oxidized aluminum data from VADE, HDR, and DHR systems at 70°

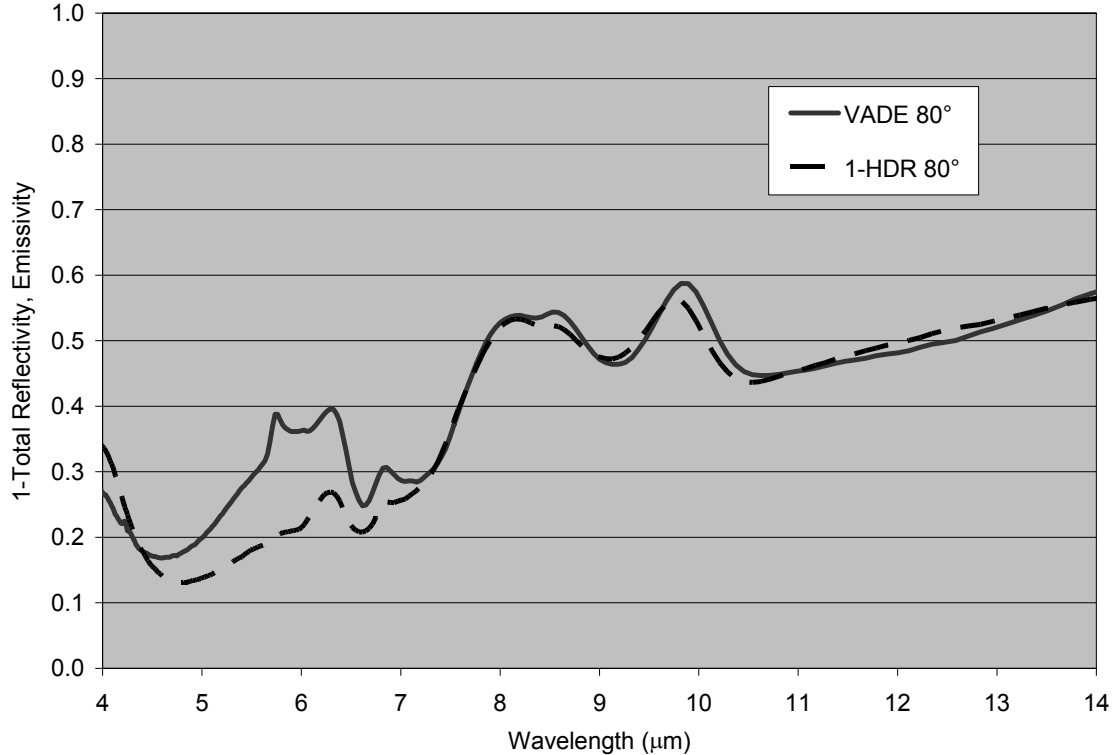


Figure 9: Comparison of oxidized aluminum data from VADE, HDR, and DHR systems at 80°

## 7. USEFULNESS OF VADE METHOD

Our VADE has recently been used to verify total reflectivity measurements when results were non-intuitive or considered suspect<sup>5</sup>. In these cases, we can have greater confidence in the data when two independent measurements agree well with modeling results. This is particularly true when working near the limits of available testing equipment.

Typical reflectometers are unable to detect backscattered light, which can be a limitation in characterizing some materials. In DHR, backscattered light that exits the source aperture is lost, either directly, or indirectly via multiple bounces. The HDR system cannot illuminate the sample from the detection angle (the reciprocal of backscatter), as the overhead mirror blocks a finite amount of the source. Direct emissivity measurements are not limited in this way, since the sample is the light source.

High-angle measurements in both reflectometers are difficult, but possible either by system modification and/or by careful alignment (including a proper aperture and sample size). Our VADE system is also limited, but this can be varied with relative ease by appropriate choice of heater temperature, sample size, cold stop aperture, and the heater block top plate which holds the sample.

## 8. CONCLUSION

We have developed a variable-angle directional emissometer that gives us great testing flexibility in situations where other equipment is incapable or would damage the sample. The system is flexible and can be adapted to meet new testing requirements or to improve signals and reduce noise. The current configuration performed well in an inter-



comparison with other equipment, showing a high level of agreement, and we have successfully used the VADE to correlate with modeling and as a “direct” verification of reflectivity data. Used as a complement to either HDR or DHR measurements, our VADE provides a more complete dataset for material characterization.

## ACKNOWLEDGMENT

Sandia is a multi-program laboratory operated by Sandia Corporation, a Lockheed Martin Company, for the United States Department of Energy’s National Nuclear Security Administration under contract DE-AC04-94AL85000.

## REFERENCES

- 
- <sup>1</sup> C. H. Seager, M.B. Sinclair, J. G. Fleming, “Accurate measurements of thermal radiation from a tungsten photonic lattice”, *Applied Physics Letters* **86**, 244105 (2005)
  - <sup>2</sup> D. B. Chase, “The Sensitivity and Limitations of Condensed Phase Infrared Emission Spectroscopy”, *Applied Spectroscopy* **35**, 77-81 (1981)
  - <sup>3</sup> J. T. Neu, M. T. Beecroft, R. Schramm, “Extended Performance Infrared Directional Reflectometer for the Measurement of Total, Diffuse and Specular Reflectance,” *Proceedings of SPIE* **2260**, 62-73 (1994)
  - <sup>4</sup> H. M. Graham, H. G. Carter, “Correction for Angular Spread in HDR Determination of IR Optical Constants”, *Proceedings of SPIE* **5192**, 80–90 (2003)
  - <sup>5</sup> S. A. Kemme, A. A. Cruz-Cabrera, D. W. Peters, A. R. Ellis, R. D. Briggs, T. R. Carter, S. Samora, “Managing Thermal Emission: Plasmon/Photon Coupling Using Diffractive Optics Technology”, *Proceedings of SPIE* **6975**, 697502 (2008)